CORONAVIRUS

Copyright © 2022 The Authors, some rights reserved; exclusive licensee American Association for the Advancement of Science. No claim to original U.S. Government Works. Distributed under a Creative Commons Attribution License 4.0 (CC BY).

Swiss public health measures associated with reduced SARS-CoV-2 transmission using genome data

Sarah A. Nadeau[1,2]*, Timothy G. Vaughan[1,2], Christiane Beckmann[3], Ivan Topolsky[1,2], Chaoran Chen[1,2], Emma Hodcroft[2,4], Tobias Schär[1], Ina Nissen[1], Natascha Santacroce[1], Elodie Burcklen[1], Pedro Ferreira[1,2], Kim Philipp Jablonski[1,2], Susana Posada-Céspedes[1,2], Vincenzo Capece[1], Sophie Seidel[1,2], Noemi Santamaria de Souza[5], Julia M. Martinez-Gomez[6], Phil Cheng[6], Philipp P. Bosshard[6], Mitchell P. Levesque[6], Verena Kufner[7], Stefan Schmutz[7], Maryam Zaheri[7], Michael Huber[7], Alexandra Trkola[7], Samuel Cordey[8], Florian Laubscher[8], Ana Rita Gonçalves[9], Sébastien Aeby[10], Trestan Pillonel[10], Damien Jacot[10], Claire Bertelli[10], Gilbert Greub[10], Karoline Leuzinger[11,12], Madlen Stange[2,12,13], Alfredo Mari[2,12,13], Tim Roloff[2,12,13], Helena Seth-Smith[2,12,13], Hans H. Hirsch[11,12], Adrian Egli[12,13], Maurice Redondo[3], Olivier Kobel[3], Christoph Noppen[3], Louis du Plessis[1,2], Niko Beerenwinkel[1,2], Richard A. Neher[2,14], Christian Beisel[1], Tanja Stadler[1,2]*

Genome sequences from evolving infectious pathogens allow quantification of case introductions and local transmission dynamics. We sequenced 11,357 severe acute respiratory syndrome coronavirus 2 (SARS-CoV-2) genomes from Switzerland in 2020—the sixth largest effort globally. Using a representative subset of these data, we estimated viral introductions to Switzerland and their persistence over the course of 2020. We contrasted these estimates with simple null models representing the absence of certain public health measures. We show that Switzerland's border closures decoupled case introductions from incidence in neighboring countries. Under a simple model, we estimate an 86 to 98% reduction in introductions during Switzerland's strictest border closures. Furthermore, the Swiss 2020 partial lockdown roughly halved the time for sampled introductions to die out. Last, we quantified local transmission dynamics once introductions into Switzerland occurred using a phylodynamic model. We found that transmission slowed 35 to 63% upon outbreak detection in summer 2020 but not in fall. This finding may indicate successful contact tracing over summer before overburdening in fall. The study highlights the added value of genome sequencing data for understanding transmission dynamics.

INTRODUCTION

Severe acute respiratory syndrome coronavirus 2 (SARS-CoV-2) genomes were collected at an unprecedented scale in 2020 (*1*) and have been extensively used to characterize transmission dynamics, in particular because genetic data contain information on the epidemiological relationships between cases. These genomic data enable the reconstruction of introductions and downstream transmission chains in the absence of contact tracing data (*2*). Where contact tracing data are available, this approach has been verified and has additionally helped with linking unassigned individuals to known transmission chains (*3*, *4*).

Several methods have been successfully used to reconstruct transmission dynamics at the onset of the coronavirus disease 2019 (COVID-19) pandemic using genetic data. Phylogenetic approaches reconstruct pathogen phylogenies and calculate relevant statistics from them without fitting any further explicit models. For example, phylogenetic reconstructions were used to show that reduced lineage size and diversity coincided with national lockdowns during the early Irish and English epidemics (*5*, *6*). In Switzerland, (*7*) linked regional superspreading events to a dominant lineage in the city of Basel using a phylogenetic reconstruction. Phylodynamic studies, on the other hand, assume that the phylogeny arises from an underlying model of transmission between hosts, possibly including additional complexities like migration of hosts between regions. This assumption enables estimation of population-level transmission dynamics from pathogen genome data. For example, (*8*–*10*) showed that public health measures reduced SARS-CoV-2 transmission rates in Israel, New Zealand, and Washington state, USA.

New models and careful considerations of potential biases are therefore required to quantify the effects of different public health measures in different regions. Here, we developed an analysis framework to quantify the association between the implementation and lifting of major public health interventions, such as border closures, lockdown measures, and contact tracing—three frontline tools in the fight against COVID-19 in 2020—on transmission dynamics. Our framework uses a two-step process that carefully

[1]Department of Biosystems Science and Engineering, ETH Zurich, 4058 Basel, Switzerland. [2]SIB Swiss Institute of Bioinformatics, 1015 Lausanne, Switzerland. [3]Viollier AG, 4123 Allschwil, Switzerland. [4]Institute for Social and Preventive Medicine, University of Bern, 3012 Bern, Switzerland. [5]Department of Biology, ETH Zurich, 8092 Zurich, Switzerland. [6]Department of Dermatology, University Hospital Zurich, University of Zurich, 8091 Zurich, Switzerland. [7]Institute of Medical Virology, University of Zurich, 8057 Zurich, Switzerland. [8]Laboratory of Virology, Department of Diagnostics, Geneva University Hospitals & Faculty of Medicine, 1205 Geneva, Switzerland. [9]Swiss National Reference Centre for Influenza, University Hospitals of Geneva, 1205 Geneva, Switzerland. [10]Institute of Microbiology, University Hospital Centre and University of Lausanne, 1011 Lausanne, Switzerland. [11]Division of Clinical Virology, University Hospital Basel, 4051 Basel, Switzerland. [12]Department of Biomedicine, University of Basel, 4031 Basel, Switzerland. [13]Division of Clinical Bacteriology and Mycology, University Hospital Basel, 4031 Basel, Switzerland. [14]Biozentrum, University of Basel, 4056 Basel, Switzerland.
*Corresponding author. Email: tanja.stadler@bsse.ethz.ch (T.S.); sarah.nadeau@bsse.ethz.ch (S.A.N.)

source: https://doi.org/10.48350/174614 | downloaded: 3.5.2024

Downloaded from https://www.science.org at Universitaetsbibliothek Bern on January 31, 2023

combines phylogenetic and phylodynamic methods to address potential sampling biases and phylogenetic uncertainty. Within the Swiss SARS-CoV-2 Sequencing Consortium (S3C) (*11*), we sequenced 11,357 Swiss SARS-CoV-2 genomes until 1 December 2020. After combining these genomes with additional data available on Global Initiative on Sharing Avian Influenza Data (GISAID) (*12*) and down-sampling to control for biases in sampling efforts over time and among geographic regions, we were left with 5520 Swiss SARS-CoV-2 genomes representing up to 5% of weekly confirmed cases in Switzerland. We used these genomes to characterize transmission dynamics in Switzerland until the emergence and widespread dissemination of more transmissible variants of concern, starting in December 2020 (*13*). Our framework allows us to identify a clear effect of border closures and the spring 2020 partial lockdown on the rate of new introductions to Switzerland and their persistence. Furthermore, we were able to quantify the degree to which local transmission slowed upon outbreak detection. We find that this effect was strongest during summer 2020, when cases were low and contact tracing efforts were likely more effective. To demonstrate the broader applicability of our analysis framework, we additionally analyzed data from New Zealand, where quarantine measures were stricter and local transmission was extremely limited throughout 2020. In New Zealand, we quantify a stronger transmission slowdown after outbreak detection, consistent with contact tracing there being highly effective.

RESULTS

Introductions and their persistence shed light on the effects of border closure and lockdown

First, we identified putatively independent introductions of SARS-CoV-2 into Switzerland and estimated their persistence. To do this, we selected SARS-CoV-2 genome sequences corresponding to up to 5% of confirmed cases each week, stratified to be geographically representative when possible (fig. S1). We divided these sequences by Pango lineage, because these lineages should represent monophyletic clades in the global SARS-CoV-2 phylogeny (*14*). Because of the hierarchical nature of Pango lineages, we aggregated lineages dominated by Swiss sequences into their respective parent lineages, allowing us to assume each analyzed lineage originated outside Switzerland (table S1). To provide global context, we additionally selected the most genetically similar sequences from abroad for each lineage. We then constructed an approximate maximum likelihood phylogeny for each such lineage of Swiss and genetically similar foreign sequences. We subsequently identified putatively independent introductions into Switzerland from these phylogenies while allowing for a fixed number of export events. We identified two plausible sets of introductions into Switzerland, resulting from two different assumptions about the ordering of transmission events at polytomies with both Swiss and non-Swiss descendants. The set of "few" introductions was generated assuming that the majority of polytomic lineages are from within-Switzerland transmission, whereas the set of "many" introductions was generated assuming that the majority are new introductions. Sensitivity analyses show that these two polytomy assumptions capture most of the uncertainty in the size and number of introductions among analyzed sequences (Supplementary Methods and Materials, section S1 and fig. S2). Using additional data on which cases were from managed isolation and quarantine facilities in New Zealand versus which were identified in the community, we show that, as expected, the "many introductions" polytomy assumption is more realistic when the probability of infection abroad is high compared with the probability of locally acquired infection (Supplementary Methods and Materials, section S2). Throughout, we report uncertainty based on the difference between the few and many introductions sets.

We estimate that the analyzed sequences originate from between 557 (few) and 2284 (many) introductions into Switzerland. These introductions were roughly power law–distributed in size (fig. S3), with the 10 largest introductions accounting for 16 to 30% of sampled genomes. Introductions that yielded more than one sampled Swiss case in our dataset tended to be geographically constrained. Between 64 (few) and 92% (many) of sampled transmission chains (introductions with >1 sample) were sampled in only 1 or 2 of the 26 Swiss cantons (fig. S4A). As expected, larger introductions were sampled in more cantons (Pearson's R between introduction size and number of cantons is 0.86 for many introductions and 0.75 for few introductions; P values for both associations are $<2.2 \times 10^{-16}$; fig. S4B). From a down-sampling analysis, we observed that if we were to include more sequences, then we would identify more introductions (fig. S2C). Therefore, the analyzed genomes do not represent all introductions into Switzerland but, given that the samples are spatiotemporally representative, are a representative subset of introductions. Because of incomplete sampling, each sampled introduction contains only a subset of all cases in the full transmission chain.

Because we sampled sequences proportionally to confirmed cases through time [coefficient of determination (R^2) between number of confirmed cases and number of analyzed Swiss sequences each week is 0.72, regression $P = 5.1 \times 10^{-13}$; fig. S1A], we can assume that trends through time in the number and persistence of introductions are representative of the underlying dynamics. Figure 1A shows the number of newly sampled introductions identified each week from our dataset, which peaked the week of 15 March under both polytomy assumptions. Switzerland closed its external borders to Italy on 13 March 2020 and to the rest of the world shortly thereafter (*15*). To disentangle the effect of the border closures versus local control measures, we back-calculated the expected number of total (both sampled and unsampled) introductions each week under a birth-death skyline (BDSKY) model (*16*). This calculation corrects for the probability that an introduction went extinct or remained unsampled each week until the end of the sampling period, given the estimates of the sampling proportion and the time-varying effective reproductive number R_e in Switzerland. Then, we developed a simple null model that assumes that, before 13 March 2020, total introductions were a linear function of case counts in Switzerland's largest neighboring countries (Italy, France, Germany, and Austria). Here, we are assuming that incidence in travelers to Switzerland followed incidence in the general community in these countries. Figure 1C shows that this model fit to total introduction estimates generated on the basis of each polytomy assumption and model projections (dashed lines) from 13 March through the partial reopening of Switzerland's European borders on 15 June 2020 (*15*). In the following, we report uncertainty based on the 95% highest posterior density (HPD) upper and lower bound estimates for R_e used to estimate total introductions. Uncertainty in travel patterns is discussed later. Compared with the null model, we estimated a reduction of 7000 (few introductions;

Downloaded from https://www.science.org at Universitaetsbibliothek Bern on January 31, 2023

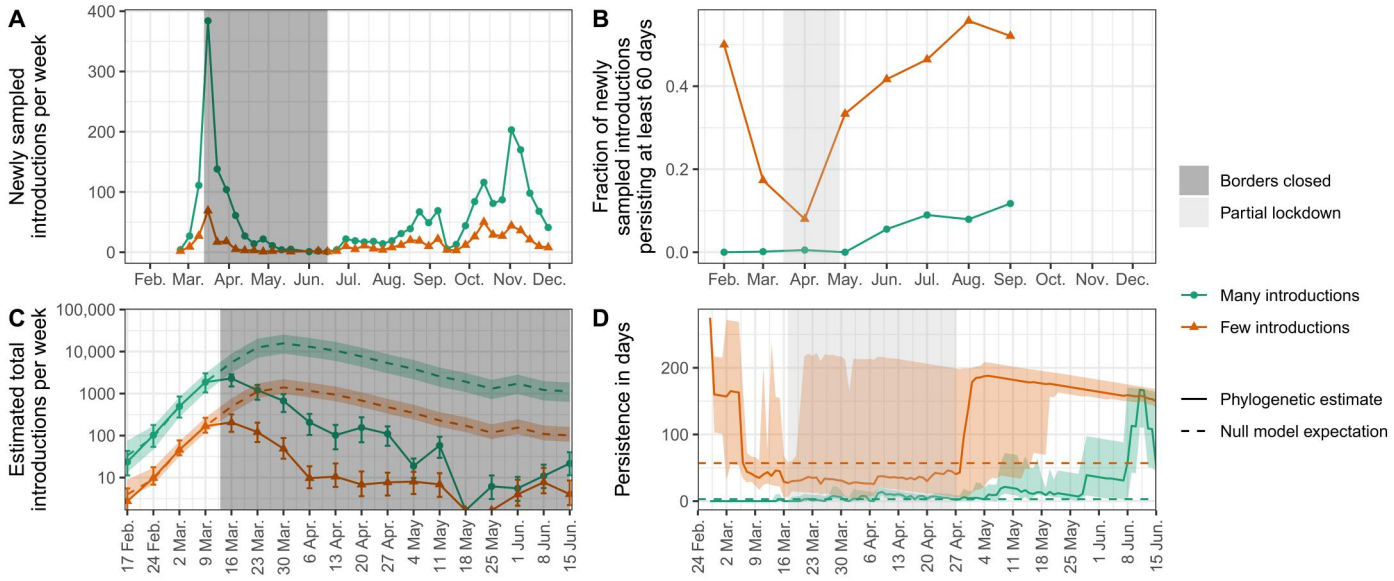

Fig. 1. Genome-based estimates of SARS-CoV-2 introductions into Switzerland and their persistence. (**A**) shows the number of newly sampled introductions identified each week, and (**B**) shows the fraction of newly sampled introductions each month that persisted for at least 60 days from the oldest to the most recent sample. This persistence measure is only defined until September because we only considered sequences obtained until 1 December 2020. Orange and green correspond to estimates generated under the few and many introductions polytomy assumptions, respectively. (**C**) and (**D**) focus on dynamics around the Swiss border closure and partial lockdown periods, which are highlighted with shaded rectangles. (C) shows estimated total introductions (solid lines) compared with a null model (dashed lines) where total introductions are a linear function of case numbers in Switzerland's neighboring countries. The null model is fit to the points before the border closure, and values after that are projections. Uncertainty bounds for total introductions (error bars) and null model predictions (colored shaded areas) are based on the 95% upper and lower HPD bounds for effective reproductive number (R_e) when estimating the total introductions. Uncertainty in travel patterns is not shown; see fig. S5. (D) shows the distribution of ongoing persistence for introductions circulating each day (solid lines) compared with a null model (dashed lines) where persistence is constant through time (equal to the median calculated until 15 June). Solid lines are median time to last sampling among introductions of newly sampled or still ongoing each day. The shaded areas show the interquartile range of this persistence distribution.

uncertainty of 4500 to 11,000) or 79,000 case introductions (many introductions; uncertainty of 41,000 to 130,000). Despite the high uncertainty in the absolute number of introductions averted depending on the polytomy assumption and the precise value of R_e in Switzerland, we estimated a consistent percentage-wise reduction of 94.1% (few introductions; uncertainty of 85.9 to 97.8%) or 94.2% (many introductions; uncertainty of 86.2 to 97.9%). We note that total European case counts peaked later than in Switzerland's neighboring countries, whereas our analysis only considered neighboring countries. Thus, the period of high import pressure may have extended longer than we assumed, depending on where most introductions were coming from (fig. S5). However, our focus on neighboring countries is supported by travel statistics. For instance, neighboring countries comprised 99% of cross-border working permits granted by Switzerland for the first quarter of 2020 (about 330,000 individuals). These countries also accounted for 36% of registered arrivals at Swiss hotels in January and February 2020 (about 450,000 individuals) (*17*). Thus, we assume that introduction dynamics are largely driven by these neighboring countries. However, our estimates of the precise reduction in imported cases depend strongly on this assumption.

New introductions cannot sustain an epidemic unless they persist in the local population. Our analysis suggests that several introductions were quite persistent in Switzerland, including one that may have persisted across our entire sampling period (fig. S6). On average, introductions persisted 5 (many introductions; SD of 16 days) to 34 days (few introductions; SD of 53 days) from the oldest to the most recent sample of each introduced lineage in our dataset. Lineage persistence until last sampling was lower during the partial lockdown (17 March to 27 April; Fig. 1, B and D) compared with summer 2020. Whereas only 0.5 to 8% of introductions in April were sampled for at least 60 days, this fraction increased to 12 to 52% in September, just before a large fall wave in Switzerland. We also developed a simple null model to assess whether the spring 2020 lockdown measures and associated behavioral changes affected the persistence of introduced lineages. Here, our null model was that persistence, measured as the time until introductions circulating each day are last sampled, does not change through time. We assumed that this delay distribution always equals the median persistence calculated over the spring period (until 15 June). Figure 1D contrasts this null model assumption with empirical persistence calculated from each day under each polytomy assumption. The distribution does vary through time, deviating from the null model. We estimated that median persistence of introductions at the start of the lockdown was less than or around the median calculated over the whole spring and rose above this null model threshold in the post-lockdown period. Quantitatively, introductions persisted roughly twice as long until last being sampled at a post-lockdown peak around 10 June compared with the start of lockdown (Fig. 1D). We note that under the few introductions assumption, persistence estimates were upper-bounded by the end of our sampling period, so the increase in persistence may also be an underestimate (Fig. 1D).

Downloaded from https://www.science.org at Universitaetsbibliothek Bern on January 31, 2023

Phylodynamic model indicates summer introductions slowed after detection

Next, we investigated local transmission dynamics once SARS-CoV-2 lineages were introduced to Switzerland in more detail. To do this, we quantified time-varying transmission dynamics in Switzerland in a Bayesian phylodynamic framework. As a base model, we used the birth-death model with serial sampling originally described in (*18*). We modified the model to condition on the previously identified few or many introductions sets, that is, sequences from each introduction have an independent origin. In a nutshell, the model assumes that once lineages are introduced, they are (i) transmitted between hosts, according to a time-varying transmission rate, which is the same across all introductions; (ii) die out upon recovery/death of the host, according to a constant becoming-uninfectious rate; and (iii) yield genome samples with a time-varying sampling proportion, which is the same across all introductions. We assumed that individuals who test positive adhere to self-isolation regulations, so that sampling corresponds to a death event for the viral lineage. Under this parameterization, R_e is a function of the transmission rate, becoming-uninfectious rate, and sampling proportion.

We developed an extension to this methodology by adding a transmission rate "damping" factor to the model, with the aim of testing whether contact tracing efforts in Switzerland slowed transmission once introductions were detected. Namely, the transmission rate was allowed to decrease by a multiplicative damping factor 2 days after an introduction was first sampled. The implementation of this factor is illustrated in Fig. 2. We used a spike-and-slab prior on the damping factor to include the possibility of no transmission slowdown. We also allowed the damping factor to vary among spring, summer, and fall 2020 periods characterized by different case numbers and testing regimes in Switzerland (Fig. 3A) (*19*). Using this model, we aimed to test whether contact tracing efforts in Switzerland slowed transmission once introductions were detected. We reasoned that test-trace-isolate can only slow transmission from shortly after the first case of an introduction tests positive but not beforehand, because beforehand the introduction was circulating cryptically. The 2-day delay aimed to account for the time between an individual giving a swab sample and having their contacts notified. Specifically, this delay consists of the time to reverse transcription polymerase chain reaction (PCR) results, which was generally below 24 hours in Swiss diagnostic laboratories (*20*), plus the time for contact tracers to reach contacts or an individual to receive and input their positive test code to the SwissCovid contact tracing app. We fit the phylodynamic model in several configurations: conditioning on either the many or few introductions set, using a bounded or an unbounded sampling proportion prior (Supplementary Methods and Materials, section S3), and with or without a transmission damping factor.

Across these model configurations, we recovered roughly the same trends in R_e as estimates based on confirmed case numbers, beginning with the first analyzed sequence from 27 February (fig. S7B). Compared with confirmed case–based estimates, we estimated a sharper decline in R_e coinciding with lockdown measures. Depending on the polytomy assumption, we estimated that R_e was 2.2 (many introductions; 95% HPD: 1.5 to 2.9) or 3.5 (few introductions; 95% HPD: 2.9 to 4.2) in the week of 9 March 2020. R_e fell to 0.3 (many introductions; 95% HPD: 0.2 to 0.4) or 0.4 (few introductions; 95% HPD: 0.2 to 0.6) in the week of 16 March (posterior median estimates with no damping factor and an unbounded sampling proportion prior). With a bounded sampling proportion, peak R_e estimates were slightly higher (fig. S7). Results in fall 2020 were highly dependent on the sampling proportion prior, where R_e estimates better matched confirmed case–based estimates when the sampling proportion was treated as a fitting parameter (that is, with an unbounded prior, resulting in unrealistic estimates of the sampling proportion; see fig. S7A).

From the model fit with a damping factor, we estimated a 35 (few introductions; 95% HPD: 29 to 41) to 63% (many introductions; 95% HPD: 56 to 70) slowdown in transmission after introductions were first sampled in summer 2020 (posterior median estimates with an unbounded sampling proportion prior). In comparison, there was little support for a slowdown effect upon the first sampling during fall 2020 (Fig. 3). These results were qualitatively robust to bounding the sampling proportion prior (fig. S8). In contrast, damping factor estimates in spring 2020 were inconsistent, depending on the polytomy assumption. Low genomic diversity in SARS-CoV-2 during this period caused high phylogenetic uncertainty (see also the differences in several selected introductions in fig. S9) (*21*). This resulted in quite different estimates for the damping factor depending on the polytomy assumption used. In summary, we report a summer 2020 "slowdown" dynamic in

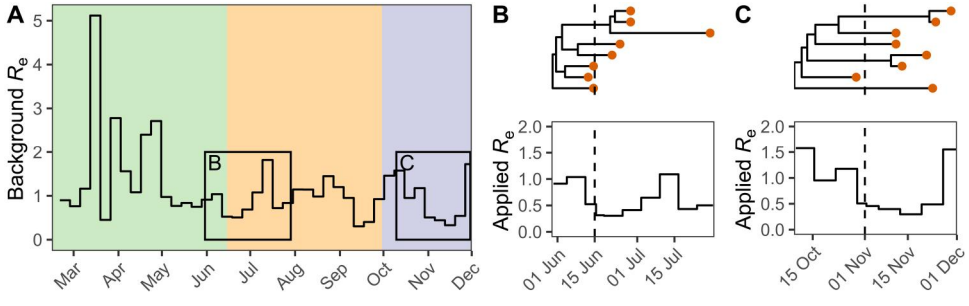

Fig. 2. Illustration of how transmission rate damping is modeled. (**A**) shows a background Swiss-wide time-varying R_e before any damping. Here, we show the median posterior result from the model applied to the many introductions data as an illustration. In each of the colored areas (green, spring; orange, summer; and purple, fall), a different damping factor is proposed. The black boxes in (A) highlight the spread of two real introductions (**B** and **C**) generated under the many introductions polytomy assumption. The genome data sampled from these introductions are shown as orange dots. The appropriate damping factor on R_e is applied to each introduction 2 days after the first genome sample (dashed lines). We used 0.6 for the summer damping factor and 0.9 for fall for this illustration. The likelihood of the genome sequence data at the tips of the phylogenies is calculated given the "applied" R_e specific to each introduction [(B) and (C), bottom].

Downloaded from https://www.science.org at Universitaetsbibliothek Bern on January 31, 2023

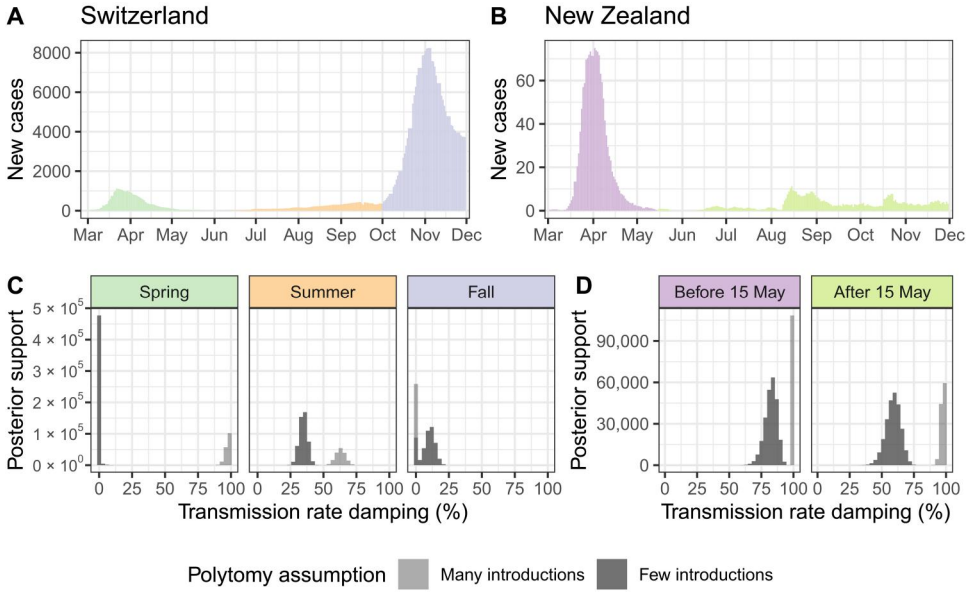

Fig. 3. Phylodynamic estimates for the transmission damping factor in Switzerland and New Zealand compared to case numbers. Case numbers in (**A**) Switzerland and (**B**) New Zealand during 2020 are shown as a 7-day rolling average of daily new confirmed cases (*47*). (**C**) and (**D**) show estimates for whether and how much transmission rates were dampened after introductions were sampled during different time periods in (C) Switzerland and (D) New Zealand. The inference was done twice: once conditioning on introductions is identified, assuming many introductions (light gray), and once assuming few introductions (dark gray). Thus, the difference between estimates in light and dark gray is due to phylogenetic uncertainty. Results shown are from the model with an unbounded sampling proportion prior; results with a bounded sampling proportion prior are similar (fig. S8).

SARS-CoV-2 transmission in Switzerland, where transmission slowed after the first genome in a new introduction is sampled. This slowdown was not observed in fall 2020.

New Zealand data show that slowdown effect is not Switzerland specific

Although Switzerland is centrally located in Europe and well connected to other countries, especially those in the (normally) barrier-free Schengen zone, New Zealand is a relatively isolated island nation. In addition, New Zealand aimed to eradicate SARS-CoV-2 throughout 2020 using strong measures such as keeping its borders closed and enforcing strict quarantine on arrival (*22*), whereas Switzerland partially reopened its borders to Europe on 15 June. We applied the same analysis framework for introduction estimation and phylodynamic inference to SARS-CoV-2 sequences from New Zealand as a comparison to our Switzerland-specific results. For the phylodynamic analysis, we estimated independent damping factors before and after an epidemic breakpoint in mid-May 2020, when local transmission was briefly eradicated (*9*, *23*). Case numbers after that were low through December 2020 (Fig. 3B) (*23*).

From the model fit with a damping factor, we estimated transmission damping in New Zealand before and after 15 May to be comparable with or stronger than in Switzerland during summer and fall 2020 (Fig. 3D) regardless of the polytomy assumption used. Thus, the existence of a transmission damping effect is not specific to Switzerland. From the model fit without a damping factor, our estimates for the sampling proportion and R_e were inconsistent. In particular, the sampling proportion was estimated to be unrealistically high when conditioning on the many introductions dataset. However, including the damping factor in the model reconciled estimates based on each polytomy assumption, yielding more realistic estimates for the sampling proportion and predamping R_e (fig. S10).

DISCUSSION

We quantified the change in cross-border and local transmission dynamics with the introduction or lifting of major public health measures in Switzerland based on genome sequence data. First, we quantified the reduction in case introductions during the period of Switzerland's strictest border closures. Travel from Italy was tightly restricted beginning 13 March and with the rest of the world beginning 16 March 2020. These measures were partially lifted on 15 June, when Switzerland reopened to European countries in the Schengen zone (*15*). We used phylogenetic estimates for the number and timing of viral introductions into Switzerland to show that newly sampled introductions peaked during the week of 15 March, coinciding with the implementation of border closures. Because of many identical or near-identical SARS-CoV-2 lineages circulating widely in Europe during spring 2020, the total number of introductions to Switzerland is highly uncertain. We considered two extreme cases encompassing most of the phylogenetic uncertainty in the size and number of introductions. We additionally corrected these estimates based on the time-varying probability that an introduction went unsampled. After disentangling the effect of border closures and local control measures in this way, we show that border closures decoupled introduction dynamics from case counts in neighboring countries. Compared with a simple null model, assuming that the incidence in travelers corresponds to the incidence in Switzerland's neighboring countries, we quantified an 86 to 98% reduction in case imports from 13 March to

Downloaded from https://www.science.org at Universitaetsbibliothek Bern on January 31, 2023

15 June. Although the decoupling of case introductions and incidence in neighboring countries is clear, our estimates for precisely how many and what fraction of introductions were averted are subject to several strong assumptions, namely, that incidence in travelers is the same as the average in the different source populations and that the majority of imported cases would have come from Switzerland's neighboring countries.

Second, we quantified the reduction in local transmission during Switzerland's partial lockdown in spring 2020 compared with the pre- and post-lockdown time period. A suite of lockdown measures, including closure of schools, nonessential shops, restaurants, and entertainment and leisure establishments, was introduced on 17 March 2020. Many nonessential shops reopened on 27 April before schools, and most other shops reopened on 11 May (*24*). We estimated that sampled introductions circulating on 17 March persisted only about half as long until last sampling as in mid-June. We also estimated that only 0.5 to 8% of newly sampled introductions in April persisted more than 60 days until last being sampled compared with 12 to 52% in September. These findings agree with previous findings (*25*), which demonstrated a reduction in the number of transmission clusters and the risk of transmission within clusters in the Canton of Vaud, Switzerland after the implementation of lockdown measures. Last, we obtained genome-based estimates for the time-varying effective reproductive number R_e in 2020 from our phylodynamic model. We estimated that R_e dropped from 2.2 to 3.5 in the week of 9 March to 0.3 to 0.4 in the week of 16 March, coinciding with lockdown measures. Two models fit to hospitalization and death (*26*) and that confirmed case (*27*) data in Switzerland gave similar or slightly lower pre-lockdown R_e estimates of 2.1 to 3.8 and 1.6 to 1.9, respectively, and similar or slightly higher post-lockdown R_e estimates of 0.3 to 0.6 and 0.6 to 0.8 after 29 March, respectively. Our phylodynamic estimates, which account for an influx of introduced cases, suggest a sharper reduction in R_e coinciding with the Swiss lockdown than these estimates based on epidemiological data. This could be due to accounting for imported cases or the case count smoothing used in (*26*, *27*).

Last, we quantified a summertime slowdown dynamic in Switzerland in which introductions initially spread faster and then slowed by 35 to 63%. This dynamic was not observable in fall 2020 in Switzerland. A plausible explanation of this dynamic is a successful test-trace-isolate implementation that roughly halved transmissions once an introduction was identified during summer 2020 in Switzerland. We cannot make a statement about the relative speed of transmission chains before and after first sampling in spring 2020. This is because many lineages are ambiguous as to whether they were imported and died out quickly or resulted in extensive, ongoing local transmission. Therefore, conditioning the birth-death phylodynamic model on few or many introductions during this period yields very different results. For the damping factor analysis, we made the strong assumption that transmission in all lineages descending from an introduction slows simultaneously 2 days after the first genome sample belonging to the introduction is collected. This may be justified if efficient informal backward contact tracing occurred or if individuals in sister lineages were identified around the same time, but their samples were not sequenced or not included in our analysis. Then, there are other possible explanatory factors at play. First, travelers returning to Switzerland during summer 2020 have been implicated in transmitting more than nontravelers (*28*). Thus, a passive transmission slowdown might have happened as introduced lineages moved into the nontraveler population. We would expect travelers in fall to have similar contact networks as those in summer, but we did not quantify a transmission slowdown in Switzerland in fall. This coincides with high case numbers during a fall wave, when Swiss contact tracing was reported to be overburdened (*29*). Second, contacts of positive cases were likely tested more intensely, potentially yielding "bursts" of samples around the first detected cases that subsequently disappeared. If so, then we can still interpret the slowdown dynamic as evidence that test-trace-isolate implementation was working, but it is difficult to determine precisely by how much transmission actually slowed.

International comparisons also lend perspective to the transmission slowdown effect that we quantify from the Swiss genome data. Using the same analysis framework, we quantified a substantial slowdown effect in New Zealand during two different time periods. Thus, this slowdown effect is not unique to Switzerland in summer 2020. One study (*4*) showed, using genome sequence data, that New Zealand contact tracing was highly effective in identifying SARS-CoV-2 infection clusters. Then, another study (*30*) exploited an accidental, partial breakdown of English contact tracing to show that normal contact tracing in early fall 2020 reduced transmissions by 63% in the 6 weeks after a positive case. This measure is within the range of our estimates for a transmission slowdown in Switzerland in summer 2020.

A primary limitation of our study is that we cannot be certain about the precise number and timing of viral introductions because of phylogenetic uncertainty and a lack of detailed, case-level data on location of exposure. We account for this uncertainty throughout by presenting results under two different many-introductions and few-introductions polytomy assumptions. However, we note that the fraction of polytomic lineages that were independent introductions likely decreased throughout spring 2020, because local incidence rose, travel declined, and the probability of locally acquired infection rose. Thus, we expect the truth to lie somewhere between the estimates generated under the two polytomy assumptions. Then, our quantitative estimates for how many and what fraction of introductions were averted by border closure measures are sensitive to our specific modeling assumptions. Last, we cannot definitively attribute the transmission slowdown effect that we quantified to contact tracing. To validate or refute our hypothesis that the transmission slowdown is linked to contact tracing, it would be interesting to study paired genomic and case-level contact tracing data should these become available.

Together, our results quantify the reduction of case importation and local transmission in Switzerland during the spring 2020 partial lockdown and partial border closure periods. Furthermore, we provide genome-based quantification of a summertime transmission slowdown in Switzerland that may be linked to successful contact tracing efforts. This slowdown was not observed in fall when contact tracing efforts were overwhelmed in Switzerland but was observed in data from New Zealand in 2020. We have shown that our inference framework is straightforward to apply to different datasets and produces quantitative estimates that we envision can help policy-makers weigh general and specific measures against the respective burdens that they impose.

Downloaded from https://www.science.org at Universitaetsbibliothek Bern on January 31, 2023

MATERIALS AND METHODS

Study design

The objective of this study was to quantify SARS-CoV-2 transmission dynamics in Switzerland over the course of the first pandemic year and to test the effects of several major public health measures on these dynamics. To do this, we investigated viral whole-genome sequences collected from individuals who tested positive for SARS-CoV-2 infection in Switzerland. We generated most of these data as part of the S3C. Sequencing of diagnostic samples by the S3C was approved by the Ethikkommission Nordwest- und Zentralschweiz, which waived ethical approval because only viral material was processed. To contextualize these data, we downloaded and analyzed additional genome sequences generously made available on the GISAID website.

The analyzed genome sequences are observational data, so we expect any biases in population testing for infection to be reflected in our data. To avoid additional bias due to uneven sequencing efforts across regions and through time, we randomly down-sampled Swiss sequences based on the number of confirmed infections in each Swiss canton each week. We chose a down-sampling threshold of 5% based on a trade-off between large sample size and spatiotemporal representativeness of the sample.

Genomic surveillance by the S3C in 2020

Together, 11,357 SARS-CoV-2 genome sequences sampled in Switzerland during 2020 were generated by the S3C (*11*). This sequencing effort represents the majority (79%) of Swiss SARS-CoV-2 genome sequences collected in 2020 and represents the sixth largest contribution of SARS-CoV-2 sequences globally in 2020 (table S2) based on data available on GISAID as of June 2022 (www.gisaid.org) (*12*). Here, we briefly describe how these samples were generated.

RNA extracts from quantitative PCR–positive patient nasal or oropharyngeal swabs were provided by Viollier AG, a Swiss medical diagnostics company. RNA was extracted using either the Abbott m2000sp or Seegene STARMag 96x4 Universal Cartridge kits. Extracts were then transferred to the Genomics Facility Basel or the Functional Genomics Center Zurich for whole-genome sequencing. Both centers used the ARTIC v3 primer scheme (*31*) to generate tiled, about 400–base pair–long amplicons. Library preparation was done with the New England Biolabs library preparation kit. Libraries were sequenced on Illumina MiSeq or NovaSeq machines, resulting in 2 × 251 base pair reads. Bioinformatics processing was performed using V-pipe (*32*), including read trimming and filtering with PRINSEQ (*33*), alignment to GenBank accession MN908947 (*34*) with the Burrows-Wheeler alignment tool (*35*), and consensus base calling. Positions with <5× coverage were masked, positions with >5% and >2 reads supporting a minor base were called with the International Union of Pure and Applied Chemistry (IUPAC) ambiguity codes, and positions with >50% reads supporting a deletion were called as a deletion. We rejected samples with <20,000 non-*N* bases. The consensus sequences are available in the GISAID repository (*12*) under submitting lab "Department of Biosystems Science and Engineering, ETH Zurich."

Dataset construction and sampling procedure

From all sequences available on GISAID (accessed on 31 May 2021), we filtered the collection date to on or before 1 December 2020 and removed nonhuman sequences and sequences <27,000 bases long. We also filtered sequences flagged by the Nextclade tool (*36*) for suspiciously clustered single-nucleotide polymorphisms (SNPs) [quality control (QC) SNP clusters status metric not "good"; ≥6 mutations in 100 bases], too many private mutations (QC private mutations status metric not good; ≥10 mutations from the nearest tree node), or overall bad quality (Nextclade QC overall status "bad"). We aligned sequences to the reference genome MN908947.3 using the multiple alignment using fast Fourier transform (MAFFT) software (*37*). Last, we followed the Nextstrain pipeline's recommendation to mask the first 100 and last 50 sites of the alignment (*38*), because the start and end of SARS-CoV-2 sequences are prone to sequencing errors (*39*).

From all available Swiss sequences, we sampled up to 5% of confirmed case counts in each Swiss canton each week until 1 December 2020. Confirmed case data were provided by the Swiss Federal Office of Public Health (now available at www.covid19.admin.ch) (fig. S1). At the time of data access, cases were only attributed at the cantonal level beginning in mid-May. Before then, we sampled randomly from across Switzerland. Where not enough sequences were available from a canton in a week, we used all available sequences. To reduce the size of the alignments for phylogenetic analysis, we divided the focal Swiss set into Pango lineages (*14*) similarly as in (*10*). Lineages composed of >50% Swiss sequences were aggregated into their parent lineage(s) until ≤50% were Swiss. This aims to ensure that each analyzed lineage originated outside of Switzerland. Table S1 lists the analyzed aggregated lineages and the number of sequences per lineage.

We then added the most genetically similar sequences from abroad to each lineage alignment to add a global context. This aimed to help distinguish between SARS-CoV-2 variants unique to Switzerland (likely within-Switzerland transmission) and variants also circulating abroad (possibly recent introductions or exports). We considered all non-Swiss sequences from each lineage available on GISAID that passed the quality-filtering steps detailed above and applied the Nextstrain priority script (*38*) to rank these sequences by their genetic similarity to Swiss sequences in each lineage alignment. Briefly, the priority script ranks a set of foreign context sequences by the Hamming distance to their nearest neighbor within a set of focal sequences. Context sequences are further penalized for having high numbers of masked positions or for being more distant neighbors of the same focal sequence. We selected twice as many context sequences as focal Swiss sequences for each analyzed lineage alignment. Our results are based on a final set of 5520 focal sequences from Switzerland and 11,009 genetically similar sequences from abroad, which were divided into 148 lineage alignments (table S1).

Phylogenetic analysis

We estimated an approximate maximum likelihood phylogeny for each lineage alignment using IQ-TREE (*40*) under a Hasegawa-Kishino-Yano (HKY) substitution model (*41*) with empirical base frequencies and four gamma rate categories to account for site-to-site heterogeneity (*42*). We added one of the earliest collected SARS-CoV-2 genomes, Wuhan/WH01/2019 (GISAID strain EPI_ISL_406798, GenBank accession: MT019529.1), as an outgroup for rooting to each alignment and estimated branch lengths in calendar time units using least-squares dating (*43*) implemented in IQ-TREE. We used a strict molecular clock and a minimum

Downloaded from https://www.science.org at Universitaetsbibliothek Bern on January 31, 2023

mutation rate of 8×10^{-4} substitutions per site per year, based on estimates by Nextstrain (*44*). We constrained the most recent common ancestor to be between 15 November and 24 December 2019, also based on estimates by Nextstrain (*44*), and set the minimum branch length to zero. Sequences that violated the strict clock assumption (*z* score threshold of >3) were removed, and near-zero length branches (<1.7×10^{-5} substitutions per site) were collapsed into polytomies, reflecting the fact that the sequence data alone were not sufficient to resolve the ordering of these transmission events. Given the root date constraints, the mutation rate conformed to the lower bound of 8×10^{-4} with extremely narrow confidence intervals. After removal of sequences violating the strict clock assumption, 5452 sequences remained across all lineage trees.

Identifying introductions

We identified putative Swiss transmission chains (collections of two or more genome sequences resulting from within-Switzerland transmissions) from each lineage tree while allowing for a fixed number of export events. We used the following criteria applied on a recursive tip-to-root tree traversal: At least two Swiss sequences are part of a clade in the tree, and the subtree spanned by these Swiss sequences is monophyletic upon removing (i) up to three export events, where (ii) only one export event may occur along each internal branch. Exports are clades containing non-Swiss sequences. We chose a conservative value for (ii) while still allowing some exports and note that the number of inferred transmission chains is robust to different values for (i) given (ii) (fig. S2A). We assumed that the identified transmission chains and remaining singleton Swiss sequences each represent an independent introduction into Switzerland.

We repeated this procedure twice for each lineage tree, making different assumptions upon reaching a polytomy where non-Swiss descendent(s) of the polytomy would cause the proposed introduction to violate criterion (i). First, we split all Swiss clades descending from the polytomy into independent introductions. The second time, we aggregated descendent Swiss clades, going in descending size order, into a single introduction. If in doing this we reached criterion (i), then we continued aggregating descendants into a second introduction and so on. The above procedures are heuristic but analogous to the accelerated transformation and delayed transformation methods for assigning character transformations when multiple scenarios are equally parsimonious (*45*). In summary, we identified introductions twice, generating estimates that represent two plausible sets of many and few introductions at polytomies, where sequence data are not informative about the order of the branching events.

Uncertainty in identifying introductions

We evaluated the effect of several variables on the number and size of identified introductions, as discussed in Supplementary Methods and Materials, section S1. We found that our two different polytomy assumptions are sufficient to capture most of the uncertainty in the number and size of introductions due to the specific heuristic criteria used to identify introductions from a phylogenetic tree (fig. S2A). As expected, increasing the ratio of foreign context to focal Swiss sequences analyzed identified more, smaller introductions compared with a lower ratio. However, our two different polytomy assumptions at a 2:1 ratio were again sufficient to capture most of this uncertainty (fig. S2B).

Quantifying the reduction of introductions during the time of border closures

Before fitting our null model for introductions through time, we back-calculated the total number of introductions each week expected under a BDSKY model, as described in the "Phylodynamic analysis" section below. Under this model, one can calculate the probability $P(t)$ that a new introduction at time t would have no sampled descendants by 1 December 2020. This formula is given in (*16*). We used weekly time bins, taking the median and 95% HPD upper and lower bounds for R_e from our phylogenetic analysis (see below), a constant sampling proportion of 5% based on our known sampling scheme, and a constant becoming-uninfectious rate of 36.5 per year, which corresponds to an average of 10 days to becoming uninfectious (roughly in line with estimates provided by the Swiss Federal Office of Public Health) (*46*). We divided the number of sampled introductions each week by $1 - P(t)$, the probability an introduction at the start of the week would yield a sampled descendant by 1 December 2020. This yielded an estimate for the total number of introductions each week (both sampled and unsampled) while accounting for varying local transmission dynamics. For a more extended description of the implementation of this correction, see Supplementary Methods and Materials, section S4.

Then, we assumed a simple null model in which introductions are a linear function of case counts in Switzerland's largest neighboring countries: Italy, France, Germany, and Austria. We used a 7-day rolling average of case count data from the European Centre for Disease Prevention and Control (ECDC) (*47*). Furthermore, we considered up to an 18-day delay between the actual introduction event and an introduction being sampled. This is based on the 8-day lag from importation to first local transmission estimated by du Plessis *et al.* (*6*) in the United Kingdom and a 10-day infectious period. We back-calculated total introductions as described above for each plausible delay value using either the median or 95% upper or lower HPD R_e estimate from our phylodynamic analysis (see below). We fit the model independently to each of these weekly estimates up to 13 March. We selected the delay yielding the best model fit (lowest root mean square error using the median R_e estimate) for each set of few or many introductions. These were 4 and 5 days, respectively. Last, we projected introductions after 13 March using the fitted model coefficients and ongoing case counts in the surrounding countries. We did not fit the model to data after border closures were partially lifted because travel behavior was still affected by risk of infection, risk of new restrictions being introduced, and ongoing stay-at-home guidance. This is apparent in data collected by the Swiss Tourism Federation, which demonstrates a marked drop in overnight stays by foreign residents in Switzerland from about 6.3 million in the winter season November 2019 to April 2020 to 3.1 million in the summer season May to October 2020 (*48*). As a sensitivity analysis, we also fit the model using confirmed cases in all non-Swiss European countries as defined in the ECDC's case count data (fig. S5) (*47*).

Quantifying the reduction of persistence of introductions during the lockdown

We developed a second simple null model to test whether the Swiss partial lockdown from 17 March to 27 April 2020 coincided with a

Downloaded from https://www.science.org at Universitaetsbibliothek Bern on January 31, 2023

change in the persistence of introductions. This null model assumes that, in the absence of measures, introductions circulating on any given day persist equally long. In other words, introductions die out (are no longer sampled) according to a delay distribution that is constant through time. For each date, we calculated the time from that date to the last sample for each introduction persisting on that date. Singleton introductions were trivially assumed to persist for 1 day. Then, we reported the median and interquartile range of this delay distribution from each date.

Phylodynamic analysis

After identifying introductions, we performed phylodynamic inference on them using the BDSKY method (*16*) in BEAST 2 (*49*). To avoid model misspecification due to the more transmissible alpha variant, we analyzed data only until 1 December 2020. We also pruned introductions to include only genomes generated by the S3C, because these were explicitly surveillance samples. This left 4136 genome sequences for phylodynamic analysis. The phylodynamic inference relies on two main models: a nucleotide substitution model describing an evolutionary process and a population dynamics model describing a transmission and sampling process. For the nucleotide substitution model, we assumed an HKY (*41*) model with four gamma rate categories to account for site-to-site rate heterogeneity (*42*). We used the default priors for kappa and the scale factor of the gamma distribution. We assumed a strict clock, with the clock rate fixed to 8×10^{-4} substitutions per site as estimated in (*44*).

For the population dynamics model, we used BDSKY (*16*). In BDSKY, the identified introductions are the result of a birth-death with sampling process parameterized by an effective reproductive number, a becoming-uninfectious rate, and a sampling proportion. As in (*10*), we inferred these population dynamical parameters jointly from the different introductions. More concretely, each introduction is assumed to result from an independent birth-death process having its own origin time but sharing all other parameters with the processes associated with the other introductions. We applied a uniform prior on the time of origin for each introduction, between 15 February and the oldest sample in the introduction. This constrained introductions to have an origin no earlier than 15 February, excluding the possibility of introductions and subsequent local transmission before the date of the first confirmed Swiss case was reported infected abroad in Italy (*50*). After 15 February, our prior expectation is a uniform rate of introductions through time. We fixed the becoming-uninfectious rate to 36.5 per year, as above. We allowed R_e to vary week to week, with an Ornstein-Uhlenbeck smoothing prior applied to the logarithm of this parameter. The stationary distribution is LogNormal(0.8, 0.5), and we applied an Exp(1) hyperprior on the relaxation parameter of the process. This prior constrains R_e to a wide range of reasonable values (95% range of 0.8 to 5.9) and penalizes large changes in R_e from week to week. Last, we allowed the sampling proportion to vary when major changes were made to the Swiss testing or genome sampling regimes (table S3). For our main analysis, we applied a broad LogUniform(10^{-4}, 1) prior on the sampling proportion, because we do not know how many individuals were truly infected. Alternatively, we also tried a LogUniform(10^{-4}, 0.05) prior, because we upper-bounded our sampling to 5% of confirmed cases each week (Supplementary Methods and Materials, section S3).

Last, we added an additional transmission damping factor to the model. This factor is a multiplicative damping of R_e applied to each introduction from 2 days after the oldest to the most recent sampling date in the introduction. Because we hypothesized that contact tracing was not functioning as well during periods of high case numbers, we estimated a separate damping factor for each of three periods: before 15 June 2020 (spring), 15 June to 30 September 2020 (summer), and 30 September to 1 December 2020 (fall). We used the same uninformative spike and slab prior for the damping factor in each period, with an inclusion probability of 0.5 and a uniform prior between 0 and 1, if included. For a description of the implementation of this model extension, see Supplementary Methods and Materials, section S4.

For each phylodynamic model configuration (bounded and unbounded sampling proportion prior, with and without the contact tracing damping factor) and set of introductions (many and few), we ran five independent Markov chain Monte Carlo chains. We discarded the first 10% of each chain as burn-in and combined the remaining samples across the five chains. We evaluated the effective sample size using Tracer (*51*) and verified that it was at least 100 for all inferred parameters.

New Zealand analysis

Genome sequence selection was done as for the Swiss analysis, except that we down-sampled available sequences from GISAID to 40% of confirmed case counts each week rather than 5%, and we used national case count numbers rather than stratified by region. Phylogenetic analysis was performed as for the Swiss data. The phylodynamic analysis was also the same, except that we assumed a constant sampling proportion through time, and for the bounded sampling proportion prior, we used a LogUniform(10^{-4}, 0.4) before match the down-sampling scheme.

Supplementary Materials

This PDF file includes:
Methods and Materials
Sections S1 to S4
Figs. S1 to S10
Tables S1 to S3

Other Supplementary Material for this manuscript includes the following:
MDAR Reproducibility Checklist

View/request a protocol for this paper from *Bio-protocol*.

REFERENCES AND NOTES

1. B. B. Oude Munnink, N. Worp, D. F. Nieuwenhuijse, R. S. Sikkema, B. Haagmans, R. A. M. Fouchier, M. Koopmans, The next phase of SARS-CoV-2 surveillance: Real-time molecular epidemiology. *Nat. Med.* **27**, 1518–1524 (2021).
2. M. U. G. Kraemer, D. A. T. Cummings, S. Funk, R. C. Reiner, N. R. Faria, O. G. Pybus, S. Cauchemez, Reconstruction and prediction of viral disease epidemics. *Epidemiol. Infect.* **147**, e34 (2018).
3. R. J. Rockett, A. Arnott, C. Lam, R. Sadsad, V. Timms, K.-A. Gray, J.-S. Eden, S. Chang, M. Gall, J. Draper, E. M. Sim, N. L. Bachmann, I. Carter, K. Basile, R. Byun, M. V. O'Sullivan, S. C.-A. Chen, S. Maddocks, T. C. Sorrell, D. E. Dwyer, E. C. Holmes, J. Kok, M. Prokopenko, V. Sintchenko, Revealing COVID-19 transmission in Australia by SARS-CoV-2 genome sequencing and agent-based modeling. *Nat. Med.* **26**, 1398–1404 (2020).
4. J. Douglas, F. K. Mendes, R. Bouckaert, D. Xie, C. L. Jiménez-Silva, C. Swanepoel, J. de Ligt, X. Ren, M. Storey, J. Hadfield, C. R. Simpson, J. L. Geoghegan, A. J. Drummond, D. Welch,

Downloaded from https://www.science.org at Universitaetsbibliothek Bern on January 31, 2023

Phylodynamics reveals the role of human travel and contact tracing in controlling the first wave of COVID-19 in four island nations. *Virus Evol.* **7**, veab052 (2021).
5. P. W. G. Mallon, F. Crispie, G. Gonzalez, W. Tinago, A. A. Garcia Leon, M. McCabe, E. de Barra, O. Yousif, J. S. Lambert, C. J. Walsh, J. G. Kenny, E. Feeney, M. Carr, P. Doran, P. D. Cotter, Whole-genome sequencing of SARS-CoV-2 in the Republic of Ireland during waves 1 and 2 of the pandemic. *medRxiv* , 2021.02.09.21251402 (2021).
6. L. du Plessis, J. T. McCrone, A. E. Zarebski, V. Hill, C. Ruis, B. Gutierrez, J. Raghwani, J. Ashworth, R. Colquhoun, T. R. Connor, N. R. Faria, B. Jackson, N. J. Loman, Á. O'Toole, S. M. Nicholls, K. V. Parag, E. Scher, T. I. Vasylyeva, E. M. Volz, A. Watts, I. I. Bogoch, K. Khan; COVID-19 Genomics UK (COG-UK) Consortium, D. M. Aanensen, M. U. G. Kraemer, A. Rambaut, O. G. Pybus, Establishment and lineage dynamics of the SARS-CoV-2 epidemic in the UK. *Science* **371**, 708–712 (2021).
7. M. Stange, A. Mari, T. Roloff, H. M. Seth-Smith, M. Schweitzer, M. Brunner, K. Leuzinger, K. K. Søgaard, A. Gensch, S. Tschudin-Sutter, S. Fuchs, J. Bielicki, H. Pargger, M. Siegemund, C. H. Nickel, R. Bingisser, M. Osthoff, S. Bassetti, R. Schneider-Sliwa, M. Battegay, H. H. Hirsch, A. Egli, SARS-CoV-2 outbreak in a tri-national urban area is dominated by a B.1 lineage variant linked to a mass gathering event. *PLOS Pathog.* **17**, e1009374 (2021).
8. D. Miller, M. A. Martin, N. Harel, O. Tirosh, T. Kustin, M. Meir, N. Sorek, S. Gefen-Halevi, S. Amit, O. Vorontsov, A. Shaag, D. Wolf, A. Peretz, Y. Shemer-Avni, D. Roif-Kaminsky, N. M. Kopelman, A. Huppert, K. Koelle, A. Stern, Full genome viral sequences inform patterns of SARS-CoV-2 spread into and within Israel. *Nat. Commun.* **11**, 5518 (2020).
9. J. L. Geoghegan, X. Ren, M. Storey, J. Hadfield, L. Jelley, S. Jefferies, J. Sherwood, S. Paine, S. Huang, J. Douglas, F. K. Mendes, A. Sporle, M. G. Baker, D. R. Murdoch, N. French, C. R. Simpson, D. Welch, A. J. Drummond, E. C. Holmes, S. Duchêne, J. de Ligt, Genomic epidemiology reveals transmission patterns and dynamics of SARS-CoV-2 in Aotearoa New Zealand. *Nat. Commun.* **11**, 6351 (2020).
10. N. F. Müller, C. Wagner, C. D. Frazar, P. Roychoudhury, J. Lee, L. H. Moncla, B. Pelle, M. Richardson, E. Ryke, H. Xie, L. Shrestha, A. Addetia, V. M. Rachleff, N. A. P. Lieberman, M.-L. Huang, R. Gautom, G. Melly, B. Hiatt, P. Dykema, A. Adler, E. Brandstetter, P. D. Han, K. Fay, M. Ilcisin, K. Lacombe, T. R. Sibley, M. Truong, C. R. Wolf, M. Boeckh, J. A. Englund, M. Famulare, B. R. Lutz, M. J. Rieder, M. Thompson, J. S. Duchin, L. M. Starita, H. Y. Chu, J. Shendure, K. R. Jerome, S. Lindquist, A. L. Greninger, D. A. Nickerson, T. Bedford, Viral genomes reveal patterns of the SARS-CoV-2 outbreak in Washington State. *Sci. Transl. Med.* **13**, eabf0202 (2021).
11. S3C, Swiss SARS-CoV-2 Sequencing Consortium (S3C) (2020); https://web.archive.org/web/20211021102940/https://bsse.ethz.ch/cevo/research/sars-cov-2/swiss-sars-cov-2-sequencing-consortium.html.
12. P. Bogner, I. Capua, D. J. Lipman, N. J. Cox, A global initiative on sharing avian flu data. *Nature* **442**, –981 (2006).
13. World Health Organization, Tracking SARS-CoV-2 variants (2021);https://web.archive.org/web/20211104163350/https://www.who.int/en/activities/tracking-SARS-CoV-2-variants.
14. A. Rambaut, E. C. Holmes, Á. O'Toole, V. Hill, J. T. McCrone, C. Ruis, L. du Plessis, O. G. Pybus, A dynamic nomenclature proposal for SARS-CoV-2 lineages to assist genomic epidemiology. *Nat. Microbiol.* **5**, 1403–1407 (2020).
15. S. Bradley, Switzerland re-opens its European borders, *swissinfo.ch* (2020); https://web.archive.org/web/20211020095340/https://www.swissinfo.ch/eng/politics/covid-19_what-s-happening-at-swiss-borders-and-airports-/45727184.
16. T. Stadler, D. Kühnert, S. Bonhoeffer, A. J. Drummond, Birth-death skyline plot reveals temporal changes of epidemic spread in HIV and hepatitis C virus (HCV). *Proc. Natl. Acad. Sci. U.S.A.* **110**, 228–233 (2013).
17. Swiss Federal Statistical Office, Federal Statistical Office (2020);www.bfs.admin.ch/bfs/en/home.html.
18. T. Stadler, Sampling-through-time in birth-death trees. *J. Theor. Biol.* **267**, 396–404 (2010).
19. Swiss Federal Office of Public Health, COVID-19 Switzerland (2021);https://web.archive.org/web/20211104165544/https://www.covid19.admin.ch/en/epidemiologic/case.
20. B. Marquis, O. Opota, K. Jaton, G. Greub, Impact of different SARS-CoV-2 assays on laboratory turnaround time. *J. Med. Microbiol.* **70**, 001280 (2021).
21. B. Morel, P. Barbera, L. Czech, B. Bettisworth, L. Hübner, S. Lutteropp, D. Serdari, E.-G. Kostaki, I. Mamais, A. M. Kozlov, P. Pavlidis, D. Paraskevis, A. Stamatakis, Phylogenetic analysis of SARS-CoV-2 data is difficult. *bioRxiv* , 2020.08.05.239046 (2020).
22. New Zealand Government, History of the COVID-19 Alert System. *Unite against COVID-19* (2021); https://web.archive.org/web/20211020111429/https://covid19.govt.nz/alert-levels-and-updates/history-of-the-covid-19-alert-system/.
23. J. L. Geoghegan, J. Douglas, X. Ren, M. Storey, J. Hadfield, O. K. Silander, N. E. Freed, L. Jelley, S. Jefferies, J. Sherwood, S. Paine, S. Huang, A. Sporle, M. G. Baker, D. R. Murdoch, A. J. Drummond, D. Welch, C. R. Simpson, N. French, E. C. Holmes, J. de Ligt, Use of genomics to track coronavirus disease outbreaks, New Zealand. *Emerg. Infect. Dis.* **27**, 1317–1322 (2021).
24. The Swiss Federal Council, Federal Council to gradually ease measures against the new coronavirus (2020); https://web.archive.org/web/20220527142858/https://www.admin.ch/gov/en/start/documentation/media-releases.msg-id-78818.html.
25. A. Ladoy, O. Opota, P.-N. Carron, I. Guessous, S. Vuilleumier, S. Joost, G. Greub, Size and duration of COVID-19 clusters go along with a high SARS-CoV-2 viral load: A spatio-temporal investigation in Vaud state, Switzerland. *Sci. Total Environ.* **787**, 147483 (2021).
26. J. C. Lemaitre, J. Perez-Saez, A. S. Azman, A. Rinaldo, J. Fellay, Assessing the impact of non-pharmaceutical interventions on SARS-CoV-2 transmission in Switzerland. *Swiss Med. Wkly.* **150**, w20295 (2020).
27. J. S. Huisman, J. Scire, D. C. Angst, J. Li, R. A. Neher, M. H. Maathuis, S. Bonhoeffer, T. Stadler, Estimation and worldwide monitoring of the effective reproductive number of SARS-CoV-2. *medRxiv* , 2020.11.26.20239368 (2021).
28. E. B. Hodcroft, M. Zuber, S. Nadeau, T. G. Vaughan, K. H. D. Crawford, C. L. Althaus, M. L. Reichmuth, J. E. Bowen, A. C. Walls, D. Corti, J. D. Bloom, D. Veesler, D. Mateo, A. Hernando, I. Comas, F. González-Candelas; SeqCOVID-SPAIN consortium, T. Stadler, R. A. Neher, Spread of a SARS-CoV-2 variant through Europe in the summer of 2020. *Nature* **595**, 707–712 (2021).
29. Keystone-SDA, Contact tracing not working properly, writes paper. *swissinfo.ch* (2020); https://web.archive.org/web/20211020105928/https://www.swissinfo.ch/eng/business/contact-tracing-not-working-properly--writes-paper/46090060.
30. T. Fetzer, T. Graeber, Measuring the scientific effectiveness of contact tracing: Evidence from a natural experiment. *Proc. Natl. Acad. Sci. U.S.A.* **118**, e2100814118 (2021).
31. The ARTIC Network, artic-ncov2019/primer_schemes/nCoV-2019/V3 at master · artic-network/artic-ncov2019. *GitHub* (2020);https://github.com/artic-network/artic-ncov2019.
32. S. Posada-Céspedes, D. Seifert, I. Topolsky, K. P. Jablonski, K. J. Metzner, N. Beerenwinkel, V-pipe: A computational pipeline for assessing viral genetic diversity from high-throughput data. *Bioinformatics* **37**, 1673–1680 (2021).
33. R. Schmieder, R. Edwards, Quality control and preprocessing of metagenomic datasets. *Bioinformatics* **27**, 863–864 (2011).
34. F. Wu, S. Zhao, B. Yu, Y.-M. Chen, W. Wang, Z.-G. Song, Y. Hu, Z.-W. Tao, J.-H. Tian, Y.-Y. Pei, M.-L. Yuan, Y.-L. Zhang, F.-H. Dai, Y. Liu, Q.-M. Wang, J.-J. Zheng, L. Xu, E. C. Holmes, Y.-Z. Zhang, A new coronavirus associated with human respiratory disease in China. *Nature* **579**, 265–269 (2020).
35. H. Li, R. Durbin, Fast and accurate short read alignment with Burrows-Wheeler transform. *Bioinformatics* **25**, 1754–1760 (2009).
36. I. Aksamentov, C. Roemer, E. Hodcroft, R. Neher, Nextclade: Clade assignment, mutation calling and quality control for viral genomes. *J. Open Source Softw.* **6**, 3773 (2021).
37. K. Katoh, K. Misawa, K.-I. Kuma, T. Miyata, MAFFT: A novel method for rapid multiple sequence alignment based on fast Fourier transform. *Nucleic Acids Res.* **30**, 3059–3066 (2002).
38. Nextstrain, nextstrain/ncov. *GitHub* (2020);https://github.com/nextstrain/ncov.
39. N. De Maio, C. Walker, R. Borges, L. Weilguny, G. Slodkowicz, N. Goldman, Issues with SARS-CoV-2 sequencing data. *Virological* (2020);https://virological.org/t/issues-with-sars-cov-2-sequencing-data/473.
40. L.-T. Nguyen, H. A. Schmidt, A. von Haeseler, B. Q. Minh, IQ-TREE: A fast and effective stochastic algorithm for estimating maximum-likelihood phylogenies. *Mol. Biol. Evol.* **32**, 268–274 (2015).
41. M. Hasegawa, H. Kishino, T. Yano, Dating of the human-ape splitting by a molecular clock of mitochondrial DNA. *J. Mol. Evol.* **22**, 160–174 (1985).
42. Z. Yang, Maximum likelihood phylogenetic estimation from DNA sequences with variable rates over sites: Approximate methods. *J. Mol. Evol.* **39**, 306–314 (1994).
43. T.-H. To, M. Jung, S. Lycett, O. Gascuel, Fast dating using least-squares criteria and algorithms. *Syst. Biol.* **65**, 82–97 (2016).
44. Nextstrain, Genomic epidemiology of SARS-CoV-2 with subsampling focused globally over the past 6 months. *Nextstrain* (2020);https://nextstrain.org/ncov/gisaid/global/6m?l=clock.
45. K. Miyakawa, H. Narushima, Lattice-theoretic properties of MPR-posets in phylogeny. *Discrete Appl. Math.* **134**, 169–192 (2004).
46. Swiss Federal Office of Public Health, Coronavirus: Frequently Asked Questions (FAQs) (2022); https://web.archive.org/web/20220527153158/https://www.bag.admin.ch/bag/en/home/krankheiten/ausbrueche-epidemien-pandemien/aktuelle-ausbrueche-epidemien/novel-cov/haeufig-gestellte-fragen.html.
47. European Centre for Disease Prevention and Control, Download historical data (to 14 December 2020) on the daily number of new reported COVID-19 cases and deaths worldwide, *European Centre for Disease Prevention and Control* (2020); www.ecdc.europa.eu/en/publications-data/download-todays-data-geographic-distribution-covid-19-cases-worldwide.
48. Schweizer Tourismus in Zahlen. *STV-FST*, www.stv-fst.ch/de/stiz.
49. R. Bouckaert, T. G. Vaughan, J. Barido-Sottani, S. Duchêne, M. Fourment, A. Gavryushkina, J. Heled, G. Jones, D. Kühnert, N. De Maio, M. Matschiner, F. K. Mendes, N. F. Müller, H. A. Ogilvie, L. du Plessis, A. Popinga, A. Rambaut, D. Rasmussen, I. Siveroni, M. A. Suchard,

Downloaded from https://www.science.org at Universitaetsbibliothek Bern on January 31, 2023

C.-H. Wu, D. Xie, C. Zhang, T. Stadler, A. J. Drummond, BEAST 2.5: An advanced software platform for Bayesian evolutionary analysis. *PLOS Comput. Biol.* **15**, e1006650 (2019).
50. Keystone-SDA, Switzerland confirms first coronavirus case. *swissinfo.ch* (2020); https://web.archive.org/web/20220525122732/ https://www.swissinfo.ch/eng/politics/covid-19_switzerland-confirms-first-coronavirus-case/45579278.
51. A. Rambaut, A. J. Drummond, D. Xie, G. Baele, M. A. Suchard, Posterior summarization in Bayesian phylogenetics using Tracer 1.7. *Syst. Biol.* **67**, 901–904 (2018).

Acknowledgments: We acknowledge the authors from the originating laboratories responsible for obtaining the specimens and the submitting laboratories where genetic sequence data were generated and shared via the GISAID Initiative, on which this research is based. J. de Ligt, D. Winter, and J. Wang provided additional information on the source of analyzed New Zealand sequences. A full acknowledgements table of the contributing groups, including the identifiers for all GISAID data used in this study, is available at https://doi.org/10.5281/zenodo.7257753. We thank J. Huisman for valuable discussions on the manuscript. **Funding:** This work was supported by the Swiss National Science Foundation grant 31CA30_196267 (TS) and ETH Zurich. **Author contributions:** S.A.N., T.G.V., and T. Stadler conceptualized the study. S.A.N., C. Beckmann, I.T., C.C., T. Schär, I.N., N.S., E.B., P.F., K.P.J., S.P.-C., S. Seidel, N.S.d.S., J.M.M.-G., P.C., P.P.B., M.P.L., V.K., S. Schmutz, M.Z., M.H., A.T., S.C., F.L., A.R.G., S.A., T.P., D.J., C. Bertelli, G.G., K.L., M.S., A.M., T.R., H.S.-S., H.H.H., A.E., N.B., and C. Beisel performed the data curation. S.A.N. and T.G.V. performed the formal analysis and created the visualizations. T. Stadler was responsible for funding acquisition, project administration, and supervision. S.A.N., T.G.V., L.d.P., E.H., R.A.N., and T. Stadler developed the methodology. V.C., M.R., O.K., and C.N. provided resources, and T.G.V. and C.C. provided software. S.A.N. and T. Stadler wrote the original draft. All authors reviewed and edited the manuscript. **Competing interests:** T. Stadler, R.A.N., and A.T. are current or former members of the Swiss National COVID-19 Science Task Force. C. Beckmann, M.R., O.K., and C.N. are employees at Viollier AG, a medical diagnostics company that performs tests for COVID-19 and other diseases. M.H., A.T., V.K., S. Schmutz, M.Z., V.C., S.C., F.L., A.R.G., R.A.N., H.H.H., K.L., C. Beckmann, M.R., O.K., C.N., N.B., and T. Stadler have contracts with the Federal Office of Public Health to support monitoring of SARS-CoV-2 spread in Switzerland. The other authors declare that they have no competing interests. **Data and materials availability:** All data associated with this study are present in the paper or the Supplementary Materials. All genome sequence data used in the analysis are available on GISAID (gisaid.org). The complete list of GISAID accession numbers used for analysis is available in the acknowledgments table at https://doi.org/10.5281/zenodo.7257753. Data generated by the Swiss SARS-CoV-2 Sequencing Consortium are available on GISAID (submitting lab: Department of Biosystems Science and Engineering, ETH Zurich). The code used to generate figures and values for the manuscript is available at https://doi.org/10.5281/zenodo.7257753. The phylogenetic analysis code is at https://doi.org/10.5281/zenodo.7257758, and the phylodynamic analysis code, including BEAST2 XML files, is at https://doi.org/10.5281/zenodo.7258644. This work is licensed under a Creative Commons Attribution 4.0 International (CC BY 4.0) license, which permits unrestricted use, distribution, and reproduction in any medium, provided that the original work is properly cited. To view a copy of this license, visit http://creativecommons.org/licenses/by/4.0/. This license does not apply to figures/photos/artwork or other content included in the article that is credited to a third party; obtain authorization from the rights holder before using this material.

Submitted 20 December 2021
Resubmitted 22 June 2022
Accepted 31 October 2022
Published First Release 8 November 2022
Final published 25 January 2023
10.1126/scitranslmed.abn7979

Downloaded from https://www.science.org at Universitaetsbibliothek Bern on January 31, 2023

Science Translational Medicine

Swiss public health measures associated with reduced SARS-CoV-2 transmission using genome data

Sarah A. Nadeau, Timothy G. Vaughan, Christiane Beckmann, Ivan Topolsky, Chaoran Chen, Emma Hodcroft, Tobias Schr, Ina Nissen, Natascha Santacroce, Elodie Burcklen, Pedro Ferreira, Kim Philipp Jablonski, Susana Posada-Cspedes, Vincenzo Capece, Sophie Seidel, Noemi Santamaria de Souza, Julia M. Martinez-Gomez, Phil Cheng, Philipp P. Bosshard, Mitchell P. Levesque, Verena Kufner, Stefan Schmutz, Maryam Zaheri, Michael Huber, Alexandra Trkola, Samuel Cordey, Florian Laubscher, Ana Rita Gonalves, Sbastien Aeby, Trestan Pillonel, Damien Jacot, Claire Bertelli, Gilbert Greub, Karoline Leuzinger, Madlen Stange, Alfredo Mari, Tim Roloff, Helena Seth-Smith, Hans H. Hirsch, Adrian Egli, Maurice Redondo, Olivier Kobel, Christoph Noppen, Louis du Plessis, Niko Beerenwinkel, Richard A. Neher, Christian Beisel, and Tanja Stadler

Sci. Transl. Med., **15** (680), eabn7979.
DOI: 10.1126/scitranslmed.abn7979

View the article online
https://www.science.org/doi/10.1126/scitranslmed.abn7979
Permissions
https://www.science.org/help/reprints-and-permissions

Downloaded from https://www.science.org at Universitaetsbibliothek Bern on January 31, 2023

Use of this article is subject to the Terms of service

Science Translational Medicine (ISSN) is published by the American Association for the Advancement of Science. 1200 New York Avenue NW, Washington, DC 20005. The title *Science Translational Medicine* is a registered trademark of AAAS.
Copyright © 2022 The Authors, some rights reserved; exclusive licensee American Association for the Advancement of Science. No claim to original U.S. Government Works. Distributed under a Creative Commons Attribution License 4.0 (CC BY).